Biophysical Journal Volume 72 April 1997 1878–1886

Dual-Color Fluorescence Cross-Correlation Spectroscopy for Multicomponent Diffusional Analysis in Solution

Petra Schwille,* Franz-Josef Meyer-Almes,# and Rudolf Rigler§

*Department of Biochemical Kinetics, Max Planck Institute for Biophysical Chemistry, D-37077 Göttingen, Germany; #EVOTEC BioSystems GmbH, D-22529 Hamburg, Germany; and §Department of Medical Biophysics MBB, Karolinska Institute, S-17177 Stockholm, Sweden

ABSTRACT The present paper describes a new experimental scheme for following diffusion and chemical reaction systems of fluorescently labeled molecules in the nanomolar concentration range by fluorescence correlation analysis. In the dual-color fluorescence cross-correlation spectroscopy provided here, the concentration and diffusion characteristics of two fluorescent species in solution as well as their reaction product can be followed in parallel. By using two differently labeled reaction partners, the selectivity to investigate the temporal evolution of reaction product is significantly increased compared to ordinary one-color fluorescence autocorrelation systems. Here we develop the theoretical and experimental basis for carrying out measurements in a confocal dual-beam fluorescence correlation spectroscopy setup and discuss conditions that are favorable for cross-correlation analysis. The measurement principle is explained for carrying out DNA-DNA renaturation kinetics with two differently labeled complementary strands. The concentration of the reaction product can be directly determined from the cross-correlation amplitude.

INTRODUCTION

In the last two decades fluctuation correlation analysis has proved to be a valuable tool for investigating dynamic processes at thermodynamic equilibrium conditions, such as diffusion or chemical reactions. Although the first theoretical description of the amplitude and the temporal decay of number fluctuations in a diffusion system is as old as Smoluchowski's concept of probability after-effects (Smoluchowski, 1916), it has taken a long time to reach a sensitivity adequate for detecting minute fluctuation events. After the introduction of light sources with high spatial and temporal stabilities (lasers), fluorescence spectroscopy became an appropriate technique for achieving the necessary sensitivity and probe selectivity. The first experiment in which fluorescence intensity fluctuations were recorded was carried out by Magde et al. (1972). Elson and Magde provided the theoretical background for the analysis of translational motion and chemical kinetics (Elson and Magde, 1974), and Ehrenberg and Rigler the analysis of rotational motion and kinetics of the excited state (Ehrenberg and Rigler, 1974). Since then, fluorescence correlation spectroscopy (FCS) has been employed to observe dynamics in several biochemical systems. It has been applied to measure translational and rotational diffusion, flow, and chemical reactions (Magde et al., 1972, 1978; Elson et al., 1974; Ehrenberg and Rigler, 1974; Aragon and Pecora, 1976). Concepts for characterizing molecular aggregation were introduced as higher order correlation analysis (Palmer and Thompson, 1987) or scanning FCS (Petersen, 1986; Berland et al., 1996). Once researchers achieved the single-molecule detection level with an epiilluminated confocal setup (Rigler and Widengren, 1990; Rigler and Mets, 1992), the signal-to-noise ratio for FCS was improved to the extent that a diffusional analysis of multicomponent systems with species of equal fluorescence wavelength and quantum yield but different molecular weights could be made (Rigler et al., 1992). Discriminating between species with different diffusion coefficients allows measurement of quantitative on-line kinetics of slow nucleic acid hybridization reactions (Kinjo and Rigler, 1995; Schwille et al., 1996) or acetylcholine-receptor interaction (Rauer et al., 1996).

In the above investigations, the correlation curve of a multicomponent system is evaluated, assuming a model of two or more diffusing components, by a Marquardt nonlinear least-squares fitting routine. Although this has been successfully carried out, extensive calibration measurements of all species must be carefully made to fix, for example, diffusion coefficients or related parameters. The controls are necessary because of the complex parameter landscape of the fitting function. The dual-color cross-correlation scheme prevents these preliminary calibration steps by introducing two spectroscopically separable fluorescence labels that allow simultaneous measurements of two reaction partners and their product. This technique is very helpful for further FCS multicomponent analyses of nucleic acid, antibody-antigen, or ligand-receptor interactions.

Cross-correlation schemes, in combination with fluorescence or dynamic laser light scattering techniques, have already been used to measure the rotational diffusion of asymmetrical particles, conformational relaxation of random coils, and association-dissociation dynamics (Kam and Rigler, 1982), as well as pairwise Coulomb interactions

Received for publication 6 November 1996 and in final form 16 December 1996.

Address reprint requests to Dr. Petra Schwille, Department of Biochemical Kinetics, Max Planck Institute for Biophysical Chemistry, Am Fassberg, D-37077 Göttingen, Germany. Tel.: +49-551-201-1436; Fax: +49-551-201-1435; E-mail: pschwil@gwdg.de.

0006-3495/97/04/1878/09 $2.00

between deionizated latex beads (Ricka and Binkert, 1989). Laminar flow specitivity of the correlation curve has been improved by cross-correlating different scattering wavelengths, thereby avoiding light phase coherence (Tong et al., 1993). This technique was extended by using two spatially separate laser beams of different colors to improve the discrimination of distance-insensitive effects such as particle rotation, and to gain sensitivity to flow direction (Xia et al., 1995). Dual-beam fluorescence cross-correlation spectroscopy for a single wavelength has been also applied to flow systems (Brinkmeier and Rigler, 1996).

Although the concept of dual-color fluorescence cross-correlation analysis has been suggested (Eigen and Rigler, 1994), the experimental realization has not been reported for two different, wavelength-separated fluorophores, with either of them being excited at absorption maximum. The present paper introduces this method for a dual-labeled nucleic acid reaction system, determining advantages and disadvantages in instrumentation and measurement and giving systematic estimates of the conditions under which the introduction of a second fluorescent species can significantly improve the fluorescence correlation analysis of multicomponent systems. Here the confocal illumination is carried out by focusing two laser beams on the same spot. Two spectral separated devices allow a wavelength-sensitive detection of the fluorescence signal from this focal volume element. The system under investigation consists of two complementary DNA strands that are singularly labeled with rhodamine green and Cy-5, respectively (spectra; see Fig. 1). In the course of renaturation, followed by diffusional auto- and cross-correlation analysis, the fraction of dual-labeled species increases. It can be shown that the amplitude of the cross-correlation curve is a very sensitive parameter for following the temporal evolution of the reaction product by suppressing the background fluorescence autocorrelation contributed from free educts.

MEASUREMENT PRINCIPLE AND SETUP

Fig. 2 shows the principle of the measurement; Fig. 3 shows the experimental setup. FCS is carried out using confocal optics, where the detection volume element is defined by epiillumination of the microscope objective. In one-photon excitation, the axial resolution must be improved by setting a pinhole as an optical field diaphragm in the image plane (Qian and Elson, 1991). To properly excite two dyes with well-separated emission wavelengths (e.g., green and red), two laser beams must be used. They are focused on the same spot, each defining an effective volume element for the corresponding dye. The two dyes are detected by different detection devices, and separation of emission light is carried out behind the pinhole by a dichroic mirror. Therefore, to gain enough space, the pinhole is imaged 1:1 to the photodiode by a biconvex lens.

The dye system under investigation is designed to have a green species (G) and a red species (R), as well as an increasing fraction of green-and-red substance (GR) due to the reaction of both partners. Whereas pure G and R should be recorded by only one detector, GR is detected in both of them (Fig. 2). Cross-correlation of the detector signals therefore is a means of measuring the reaction product GR independently of fluorescent educts. The cross-correlation measurement provides an improvement over the well-known case that only one of the reaction partners is fluorescently labeled, where such separation is not possible. In contrast to single-color autocorrelation analysis, the method in principle yields a yes-or-no decision about the presence of a doubly labeled reaction product, without the necessity of a mathematical evaluation of the correlation curve.

THEORY

In contrast to many fluorescence spectroscopy applications, the idea of FCS is not to analyze the temporal or ensemble

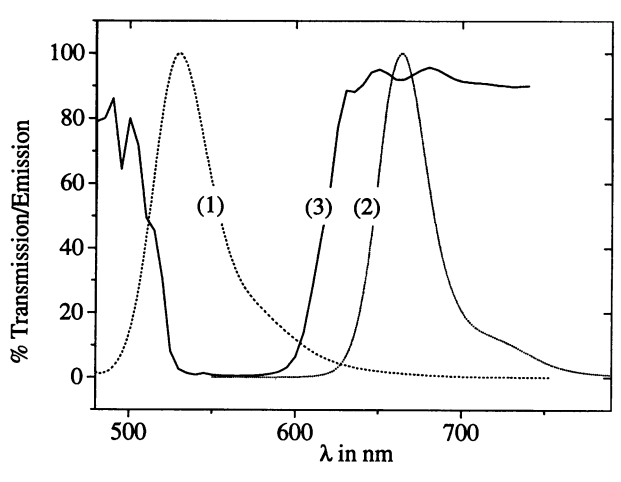

FIGURE 1 Emission spectra of rhodamin green (1) and Cy-5 (2), as well as transmission characteristics of second dichroic mirror (3).

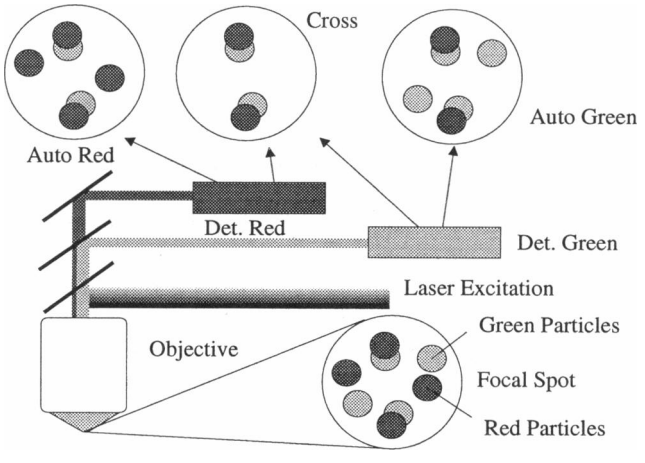

FIGURE 2 Schematic of measurement principle. Green and red lasers illuminate the sample, which contains diffusing species R, G, and GR. Photodiode DR detects R and GR; photodiode DG detects G and GR.

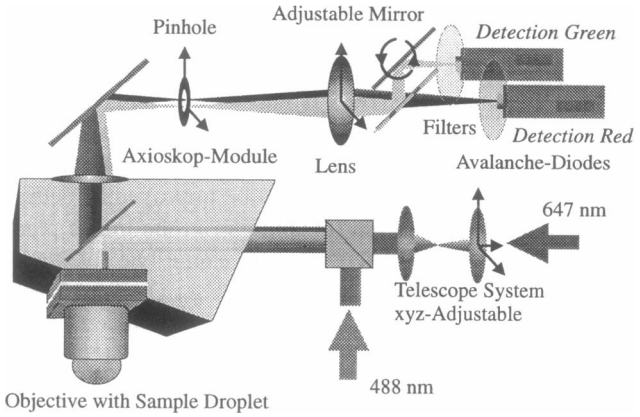

FIGURE 3 Cross-correlation setup, including Zeiss Axioskop Module with first dichroic mirror and 40 × 0.9 Plan Neofluar objective, and a second dichroic mirror in front of the "red" detector. A telescope system is used to adjust the size of the red laser beam.

average of a fluorescent sample, but to investigate the fluctuations in light emission. By autocorrelating the intensity signal (i.e., comparing the intensity values at different times), one can extract the decay constants of temporally limited processes, such as reaction relaxation rates or diffusional motions through predefined geometries. For probes in thermodynamic equilibrium, if no further effects on fluorescence are present, fluctuations arise from statistical changes in the particle number density in the detected volume element due to random Brownian processes. This is the case for the system treated here (for a review see Thompson, 1991; Rigler et al., 1992).

Consider the fluorescence intensity signal $F_i(t)$ of the fluorescent species i from a laser-illuminated volume element V. For time scales when the intensity of excitation light and fluorescence emission of the particles can considered to be constant, temporal changes will only arise from changes in concentration, and the fluctuation term $\delta F_i(t)$ is given by

$$\delta F_i(t) = \kappa_i Q_i \int_V I_{ex}(\underline{r})\mathrm{CEF}_i(\underline{r})\delta C_i(\underline{r}, t)\cdot \mathrm{d}V. \qquad (1)$$

$C_i(r, t)$ is the number density of species i at time t in the observed volume, and $I_{ex,i}$ defines the geometry of the excition beam. CEF_i stands for collection efficiency function; in confocal geometry it is given by the imaging properties of detection optics, objective, and pinhole (Qian and Elson, 1991; Rigler et al., 1993). The CEF is wavelength-dependent and must be indexed in multicolor systems. $I_{ex,i}$ is another wavelength-dependent parameter; the lasers chosen must be able to properly excite every fluorescent species. This is accomplished by using separate beams. Q_i and κ_i are constants for the molecular quantum yield and for the detection efficiency (photodiode, filters) of different fluorescent species. We can combine $I_{ex,i}(r)$, $\mathrm{CEF}_i(r)$, Q_i, and κ_i into a single parameter called the "emission characteristics" $E_i(r)$ with amplitudes η_i for every fluorophore located at r in the observed volume. The unit of η_i is photons per molecule and second:

$$\begin{aligned} E_i(\underline{r}) &= Q_i\kappa_i \cdot I_{ex,i}(\underline{r}) \cdot \mathrm{CEF}_i(\underline{r}) \\ &= \eta_i \mathrm{MDE}(\underline{r}). \end{aligned} \qquad (2)$$

MDE denotes the molecule detection efficiency in the observed volume, with values between 0 and 1 (Rigler et al., 1993). The spatial distribution of MDE is approximated as a Gaussian in lateral and axial directions within the observed volume element; therefore the integration is carried out over the whole space.

The normalized autocorrelation function for the intensity signal of a single species i is given by

$$G_{ii}(\tau) = \langle \delta F_i(t)\delta F_i(t+\tau)\rangle / \langle F_i(t)\rangle^2. \qquad (3)$$

With the above abbreviations we get the expression

$$G_{ii}(\tau) = \frac{\iint E_i(r)E_i(r')\langle \delta C_i(\underline{r}, 0)\delta C_i(\underline{r}', \tau)\rangle \mathrm{d}V\,\mathrm{d}V'}{(\langle C\rangle \int E_i(\underline{r})\mathrm{d}V)^2}. \qquad (4)$$

For a species with diffusion coefficient D_i, the number density autocorrelation term

$$\langle \delta C_i(\underline{r}, 0)\delta C_i(\underline{r}', \tau)\rangle$$

is given by

$$\langle \delta C_i(\underline{r}, 0)\delta C_i(\underline{r}', \tau)\rangle = \langle C_i\rangle (4\pi D\tau)^{-3/2} \exp(-(\underline{r} - \underline{r}')^2/4D_i\tau). \qquad (5)$$

This leads to the expression for the normalized three-dimensional diffusional autocorrelation function for species i with a Gaussian emission light distribution, lateral and axial $1/e^2$ distances r_o and z_0:

$$E_i(\underline{r}) = \eta_i \exp(-2(x^2 + y^2)/r_0^2)\exp(-2z^2/z_0^2) \qquad (6)$$

$$G_{ii}(\tau) = V_{\mathrm{eff}}^{-1}\langle C_i\rangle^{-1}(1 + \tau/\tau_{d,i})^{-1}(1 + r_0^2\tau/z_0^2\tau_{d,i})^{-1/2} \qquad (7)$$

(Aragon and Pecora, 1976; Rigler et al., 1992). V_{eff} turns out to be an effective detection volume element given by $V_{\mathrm{eff}} = \pi^{3/2}r_0^2z_0$, whereas $\tau_{d,i} = r_0^2/4D_i$ defines the average time for detected molecules of species i to diffuse out of this volume. We abbreviate the temporal fluctuation decay function of each diffusing species by

$$Diff_i \equiv (1 + \tau/\tau_{d,i})^{-1}(1 + r_0^2\tau/z_0^2\tau_{d,i})^{-1/2}.$$

If more than one noninteracting species is detected by the same detection device, the autocorrelation function is just the sum of the single contributions. For the special case of equal emission characteristics E_i for the different components (i.e., same marker fluorophor, different molecular weights), the normalized correlation function is given by

$$G_{tot} = \sum_i \langle C_i\rangle Diff_i / V_{\mathrm{eff}}(\sum_i \langle C_i\rangle)^2 = N_{tot}^{-1} \sum_i Y_i Diff_i. \qquad (8)$$

In this case, all components contribute to the time decay signal, weighted by their relative concentration fractions

$Y_i = \langle C_i \rangle / \Sigma_i \langle C_i \rangle$, whereas the amplitude of G_{tot} for $\tau = 0$ is given by the total number of fluorophores in the effective volume element $N_{tot} = V_{eff} \Sigma_i \langle C_i \rangle$. As mentioned above, for reliable quantitative evaluation of the fractions Y_i from this curve, all diffusion times $\tau_{d,i}$ should be known, and vice versa.

If the dyes undergo singlet-triplet transitions, which is very likely in the used system, for better fitting of the curves, G_{tot} must be multiplied by a triplet correction term (Widengren et al., 1994). The fitting functions are then given by

$$G_{tot,T} = (1 - T + T \cdot e^{-t/\tau_T}) \cdot G_{tot}, \tag{9}$$

where T is the average fraction of dye molecules in the triplet state with relaxation time τ_T.

In the system presented here, there are two seperate detection devices DG and DR for a probe containing fluorescent species G and R; double-labeled species GR is present at an unknown fraction and is detected by both detectors. The contributions of the fluorescence fluctuations in either detection unit will then be

$$\delta F_{DG}(t) = \int E_G(\underline{r}) \delta C_G(\underline{r}, t) dV + \int E_G(\underline{r}) \delta C_{GR}(\underline{r}, t) dV$$

$$\delta F_{DR}(t) = \int E_R(\underline{r}) \delta C_R(\underline{r}, t) dV + \int E_R(\underline{r}) \delta C_{GR}(\underline{r}, t) dV. \tag{10}$$

Autocorrelation can be carried out for both detection signals as well as the cross-correlation between them. In pure diffusional systems, where components G, R, and GR are not interacting in the time scale of detection, the distinct concentration correlation terms are set to zero: $\langle \delta C_i(\underline{r}, 0) \cdot \delta C_j(\underline{r}', t) \rangle = 0$, for $i \neq j$.

This cross-correlation measurement principle is different from the method introduced by Ricka and Binkert. By cross-correlating the species' intensity signals, they extracted the distinct terms, because $\langle \delta C_i(\underline{r}, 0) \cdot \delta C_i(\underline{r}', t) \rangle \neq 0$, due to pairwise interacting particles. If these interactions are not present, carrying out the cross-correlation yields another self term, given by the isolated autocorrelation contribution of pure species GR. For the special case in which the emission characteristics $E_i(r)$ are equal, we get the following expressions for auto- and cross-correlation functions:

$$G_{DG}(\tau) = (\langle C_G \rangle Diff_G + \langle C_{GR} \rangle Diff_{GR}) / [V_{eff}(\langle C_G \rangle + \langle C_{GR} \rangle)^2]$$

$$G_{DR}(\tau) = (\langle C_R \rangle Diff_R + \langle C_{GR} \rangle Diff_{GR}) / [V_{eff}(\langle C_R \rangle + \langle C_{GR} \rangle)^2]$$

$$G^{\times}_{DGDR}(\tau) = \langle C_{GR} \rangle Diff_{GR} / [V_{eff}(\langle C_G \rangle + \langle C_{GR} \rangle)(\langle C_R \rangle + \langle C_{GR} \rangle)]. \tag{11}$$

We see in the ideal case that the only cross-talk between the two detection units is given by the signal of doubly labeled species GR; the $G^{\times}$ temporal decay in contrast to the autocorrelation functions is governed only by the diffusion properties of GR, $Diff_{GR}$. By reaction of G and R to GR, the cross-correlation amplitude $G^{\times}(0)$ is directly proportional to the concentration of GR, because the denominator, given by the sum of product and educt, remains constant in time.

Comparing the numerators, however, it can be shown that the amplitude of the cross-correlation function will always be lower than or equal to (for the case where only species GR is present in the volume) the two autocorrelation amplitudes. Because correlation amplitudes below 0.001 are too noisy to be analyzed properly (see Thompson, 1991), there is a lower limit for detectable GR fractions, and therefore this is of great practical relevance.

NONIDEALITIES, GENERAL CASES

It has been shown that under ideal conditions, product species GR can be completely separated from the educts using cross-correlation; the temporal decay of the cross-correlation function represents only GR diffusion. Considering equal emission intensity characteristics $E_i(r)$, the effective detection volume V_{eff} is the same for both devices. Therefore, if only GR is present in the system, the three curves in Eq. 11 are identical. Actually, this need not be the case. Because $E_i(r)$ is a convolution product of excitation light and detection optics, the setup may cause differences for different species i, e.g., by using more than one laser to excite the fluorophores G and R. In this case the effective volume element and the diffusional decay $Diff_i$ must be modified. Let E_G and E_R be different in size,

$$E_G(\underline{r}) = \eta_G \exp(-2(x^2 + y^2)/r_G^2) \exp(-2z^2/z_G^2)$$

$$E_R(\underline{r}) = \eta_R \exp(-2(x^2 + y^2)/r_R^2) \exp(-2z^2/z_R^2),$$

The effective volume elements and diffusion times for the three correlation functions are given by (i denoting the detectable species):

autocorrelation DG:

$$V_{eff} = \pi^{3/2} r_G^2 z_G \quad \tau_{d,i} = r_G^2/4D_i \quad \text{(species G, GR)}$$

autocorrelation DR:

$$V_{eff} = \pi^{3/2} r_R^2 z_R \quad \tau_{d,i} = r_R^2/4D_i \quad \text{(species R, GR)}$$

cross-correlation DADB:

$$V_{eff} = \pi^{3/2}(r_G^2 + r_R^2)(z_G^2 + z_R^2)^{1/2}/2^{3/2}$$

$$\tau_{d,i} = (r_G^2 + r_R^2)/(4D_i \cdot 2) \quad \text{(species GR)}$$

If only species GR is present in this case, the correlation amplitudes $G(t = 0)$ are related as their $1/V_{eff}$. Therefore, when different laser spot sizes are used, the cross-correlation curve lies between the two autocorrelation curves. It is still possible to separate GR, but the ratio of diffusion times no longer simply represents the ratio of inverse diffusion coefficients.

In nonideal systems there will be a considerable amount of additional detection unit cross-talk due to the broad

absorption and emission spectra of the used dyes. Because our optical setup is worked out for excitation and emission in the visible spectral range, it is hardly possible to find perfectly separable dyes with adequate photophysical properties. It must be taken into account that both dyes may be excited to some extent by both lasers and emit in both spectral detection ranges. Theoretically, there are $2^3 = 8$ emission characteristics $E_i(r)$ that must be considered; in the case of focal overlap they differ at least in their amplitudes η_i. In our case of the red and green absorption/emission scenario, we can define the following (first index: emission; second index: dye; third index: excitation):

η_{GGG}, η_{RGG}: Green and red emission of green dye excited by green laser

η_{GRG}, η_{RRG}: Green and red emission of red dye excited by green laser

η_{GRR}, η_{RRR}: Green and red emission of red dye excited by red laser

η_{GGR} and η_{RGR} can be set to zero, because the green dye is proved not to be excitable by the used red laser. Although present in our system, the green anti-Stokes fluorescence of the Cy-5 is very weak; therefore we may also approximate $\eta_{GRG} \approx 0$ and $\eta_{GRR} \approx 0$.

We have to modify Eq. 10 and get the following expressions for the detected fluorescence fluctuations of species R, G, and RG:

$$\delta F_{DG}(t) = \int E_{GGG}(\underline{r})\delta C_G(\underline{r}, t)dV + \int E_{GGG}(\underline{r})\delta C_{GR}(\underline{r}, t)dV$$

$$\delta F_{DR}(t) = \int (E_{RRG}(\underline{r}) + E_{RRR}(\underline{r}))\delta C_R(\underline{r}, t)dV + \int (E_{RGG}(\underline{r}) + E_{RRG}(\underline{r}) + E_{RRR}(\underline{r}))\delta C_{GR}(\underline{r}, t)dV + \int E_{RGG}(\underline{r})\delta C_G(\underline{r}, t)dV, \quad (12)$$

resulting in much more complex correlation functions. The most obvious effect in contrast to the ideal case is that the green dye spills over into the cross-correlation term, thereby preventing a complete separation of species GR. However, the weighting factors η_i are multiplied by correlation, allowing a good suppression of single-labeled species $Diff_G$ in the cross-correlation time dependence. For equal dimensions but different amplitudes of E_i, the relative contribution to the correlation curve Eq. 8 of $Diff_G$ against $Diff_{GR}$ is given by

$$\langle \delta C_G \cdot \delta C_G \rangle / \langle \delta C_{GR} \cdot \delta C_{GR} \rangle = \eta_{RGG}/(\eta_{RGG} + \eta_{RRG} + \eta_{RRR}).$$

To give an estimation of the conditions under which the cross-correlation of different dyes is favorable against the autocorrelation of equally labeled reaction educts, we must consider the relative representation of single labels against double labels. The dual-beam setup causes some difficulties and must therefore be a real improvement compared to the case where each reaction partner carries the same dye, where the reaction just doubles the quantum efficiency of the product molecule.

In the single-color autocorrelation curve of this case, the twice-labeled species will dominate 4 times over the single labeled because of the square dependence of the autocorrelation function on molecular quantum yields (see Thompson, 1991). Therefore, an improvement by dual-color cross-correlation setup is only given if the following condition is fulfilled:

$$(\eta_{RGG} + \eta_{RRG} + \eta_{RRR})/\eta_{RGG} > 4.$$

In fact, this can be achieved with a proper dye system, so that the cross-talk nonidealities can easily be suppressed.

The effect of cross-talk between the green dye's fluorescence signals due to internal cross-correlation, however, is important to the choice of laser spot size. The greater the overlap of laser spot size $I_{ex,i}$, the less the disturbance of single-labeled species in the cross-correlation term, under the condition that the detection characteristics (CEF_i) are equal in either device. In the setup described here, we can assume approximately equal CEF_G and CEF_R, so that laser overlap should be maximized and the $E_i(r)$ are different only in amplitude η.

MATERIALS AND METHODS

Experimental setup

Fig. 3 shows the experimental setup. The 488-nm line of an argon ion laser AR 909 (Polytec, Waldbronn, Germany) and the 647-nm line of a krypton-argon ion laser Innova 90K (Coherent, Palo Alto, CA) are combined by an external dichroic mirror 530DRLP02 (Omega Optical, Brattleboro, VT). The 488-nm beam is not prefocused, the 647 beam size is increased by a parallel optics telescope system consisting of a Plan-Neofluar objective 2.5× against a Plan Neofluar objective 10× (Carl Zeiss, Oberkochen, Germany), to achieve identical focal spot size. After being reflected by a dichroic mirror 505DRLP02 (Omega Optical), the two beams epiilluminate a Plan Neofluar 40 × 0.9 Objective (Zeiss) with variable immersion liquid, set to water immersion in our case. Beam diameter $1/e^2$ values at the objective back aperture are 3.5 mm (488) and 5 mm (647), giving a Gaussian focal spot diameter r_0 of 0.7 μm for both wavelengths. The axial dimension z_0 is known from calibration measurements with pure dye rhodamine 6G. The fraction z_0/r_0 for the given setup is 5, yielding an effective volume element V_{eff} of $\sim 10^{-15}$ liter. At nanomolar concentrations, therefore, the average number of molecules in the focal spot is of the order of 1.

The fluorescence light traverses the dichroic mirror being focused by a infinity optics Axioskop lens (Zeiss) with a focal length of 164.5 mm. A pinhole of 50 μm diameter is located in the image plane, which is again imaged to the photodiode 1:1 by a 60-mm lens. Behind this lens, the fluorescent light is split by another 620DRLP02 dichroic mirror (Omega Optical) in Fig. 2, and the green spectral light is reflected by a plane mirror. Pinhole, lens, and plane mirror are independently adjustable. Additional detection light specificity is achieved with a 530DF45 (Omega) bandpass filter (green detector) and a 667EFLP (Omega) long-pass filter (red detector). For detection, we use avalanche photodiodes (SPCM-200; EG&G Optoelectronics, Canada). The photocount signal is autocorrelated over 30–120 s by a PC ALV-5000 multiple-τ correlator card (ALV, Langen, Germany), with quasilogarithmic lag times between 200 ns and 1 h. This correlator allows for auto- or cross-correlation mode; the curves as well as the intensity signal can be followed online on a PC monitor, making adjustment and signal control quite comfortable. Evaluation of the curves

can be carried out with a Marquardt nonlinear least-squares fitting routine of the correlation curves, using the diffusional one- or two-component model ($\Sigma i = 1$ or 2) with triplet correction (Eq. 9).

Biochemical system

Two oligonucleotides, one labeled with rhodamin green (excitation maximum 510 nm; Molecular Probes, Eugene, OR) and the other labeled with Cy-5 (excitation maximum 650 nm; Amersham Life Sciences, Little Chalfont, England) were synthesized by NAPS (Göttingen). The sequences were chosen as follows:

Cy5–5′-GCC GTC TCT GAC TGC TGA TGA CTA CTA TCG TAT AGT GCG G-3′ and

RhGr-5′-CCG CAC TAT ACG ATA GTA GTC ATC AGC AGT CAG AGA CGG C-3′

Both oligonucleotides were labeled at their 5′ end; thus the dyes situated at opposite sides of the double-stranded duplex (40 nucleotides long) prevented energy transfer between the two attached dye molecules. FCS analysis proved the presence of nonconjugated fluorescent dye molecules. To create a highly purified reference probe for the instrumental setup and evaluation of cross-correlation experiments, the twice-labeled DNA double strand was extensively purified. However, with a proper cross-correlation setup, the presence of pure dye does not interfere with quantitative analysis of the renaturation process. Precipitation, size exclusion chromatography, and reverse-phase high-performance liquid chromatography of single-strand oligonucleotides were not efficient enough to completely remove free dye molecules from the labeled DNA probes, a phenomenon that has been described by Aurup et al. for single-stranded rhodamine-labeled RNA molecules (Aurup at al., 1994). The free rhodamine could only be removed completely by hybridizing the single strands and separating the double-stranded RNA molecule using gel electrophoresis. We modified their protocol slightly and applied it to the purification of the double-labeled DNA double strand.

To get a standard for renaturation endpoint, the labeled complementary oligonucleotides (each 20 nM) were hybridized in the presence of 40 mM Tris, 150 mM NaCl (pH 8.0). The solution was heated in a PCR Cycler (Perkin-Elmer Applied Biosystems, Foster City, CA) for 1 min at 90°C, rapidly cooled to 75°C, and gradually cooled down to 40°C within 210 min. The DNA double strand was purified by gel electrophoresis in a 15% nondenaturating polyacrylamide gel. Electrophoresis was carried out in 89 mM Tris borate and 0.2 mM EDTA (pH 8.3). Spectroscopic analysis of the labeled DNA double strand revealed a ratio of RHGreen:Cy5:DNA of 1.1:1.0:1.3 using molar extinction coefficients of ϵ_{500} (RhGr) = 54,000 $cm^{-1}M^{-1}$, ϵ_{647} (Cy5) = 250,000 $cm^{-1}M^{-1}$, ϵ_{260} (40-bp DNA single strand) = 260,000 $cm^{-1}M^{-1}$ (Fasman, 1976), respectively. The ratio of dye absorption at 260 nm to the DNA absorption was considered. Renaturation was carried out in a droplet of annealing buffer at 22°C under the objective. Complementary oligonucleotides (10 nM of each) were mixed and subsequently measured by FCS. The reaction was followed online over 1 h, with single measurements taken every 5–10 min.

Calibration measurements

To calibrate the setup, we must determine all emission properties η_i of each fluorescence species, as well as show that the laser spot and detection volume overlap adequately. To test the chromatic correction of the measurement objective, it must be shown that the green and the red detectors "see" exactly the same spot volume. This can be done by exciting only the green dye with a 488-nm laser beam. Because the concentration of green dye is the same for both detection wavelengths, the autocorrelation functions G_{DG} and G_{DR} calculated from red and green detection intensity signals (Eq. 12) must be equal, whereas the different intensity signal amplitudes represent η_{GGG} and η_{RGG}. By comparing the two autocorrelation curves, the equal size of detection volumes can be tested. In next step we must control the spatial localization, making sure that the detection volumes of same size (tested in the above calibration) are perfectly overlapped. This can be done by cross-correlating the red and green fluorescence signals of the green dye. If the cross-correlation curve equals both autocorrelation curves, we have guaranteed this overlap. If the cross-correlation amplitude is lower than that of the two autocorrelation signals, this means that the two detectors will not see exactly the same spacial region, and fluorescence from some molecules will contribute only to one detector.

In the next step we must maximize the overlap of the two laser beams and thereby determine the values η_{RRG} and η_{RRR}. Therefore, the red dye is first excited by the red beam and detected by the "red" armed detector, then excited by the green beam and again detected in the red. Both correlation curve amplitudes and decay times must be equal if the lasers illuminate the same region, because the concentration of the dye stays the same. The fluorescence intensities measured in either case then give η_{RRR} and η_{RRG}.

After the calibration procedures, the cross-correlation setup is well defined and the measured signals are described by the above theory (Eq. 11). If the conditions cannot be fulfilled and the volume elements differ significantly, a proper quantitative evaluation of the cross-correlation data will become more complicated.

RESULTS

The calibration measurements show a very good overlap of detection and illumination volume elements with the chosen Zeiss Plan Neofluar 40 × 0.9 objective. In Fig. 4 *A*, autocorrelation of the green and red emission of rhodamine green is shown, as well as the cross-correlation curve. All curves are exactly equal; only the statistical quality differs, because of the different photon efficiencies of the dye in the two separate spectral ranges (this dependence has been quantified by Koppel, 1974). However, the curves are not equal for all objectives. Fig. 4 *B* shows the same solution, measured with a 63 × 1.2 water immersion Zeiss Plan Neofluar objective (this particular objective is no longer commercially available). The autocorrelation curves from green and red detector devices are still the same, but the cross-correlation is not. The reason for this seems to be an inefficient chromatic correction of this special objective; the detection volume elements are of the same size but are not perfectly overlapped. The choice of the objective is critical; cross-correlation turns out to be a good proof of efficiency of correction against chromatic aberrations.

Laser overlap can be well achieved by exciting the red dye with both wavelengths, although the absorbance of green light is weak. Fig. 5 shows the red spectral autocorrelation curves of Cy-5 dye with the two excitation alternatives; both curves are perfectly equal in shape. To achieve similar photon detection efficiencies of rhodamine green and Cy-5, the excitation intensities are set to 0.6 mW at 647 nm and 2 mW at 488 nm. We get the following fractions: $\eta_{GGG}/\eta_{RRR} \approx 1$, $\eta_{GGG}/\eta_{RGG} \approx 20$, $\eta_{RRR}/\eta_{RRG} \approx 8$. The critical value $(\eta_{RGG} + \eta_{RRG} + \eta_{RRR})/\eta_{RGG}$ then equals ~20, which makes the relative contribution of the green dye's fluorescence to the red detection channel negligible. We can be sure that GR is virtually the only species represented by the cross-correlation curve. Table 1 compares the measured photocounts per molecule, represented by η_i.

How well the cross-correlation works isolating species GR can be seen in Fig. 6. Here, in a mixture of green- and red-labeled single-strand DNA, as well as an unknown

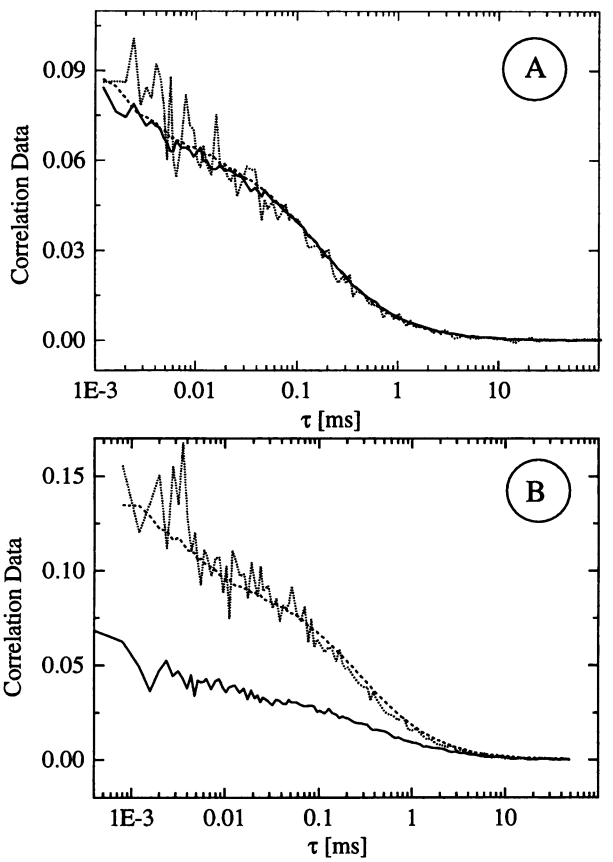

FIGURE 4 Autocorrelation curves for red (*short dots*) and green (*dots*) detector signal and cross-correlation curve (*solid line*). Rhodamin green excited at 488 nm (*A*) for Plan Neofluar 40 × 0.9; (*B*) for Plan Neofluar 63 × 1.2. One can easily see the nonideal overlap of the detection volumes in *B*: the cross-correlation amplitude is much lower than the two autocorrelation curves, which implies that there are a considerable number of molecules to be seen in only one detector.

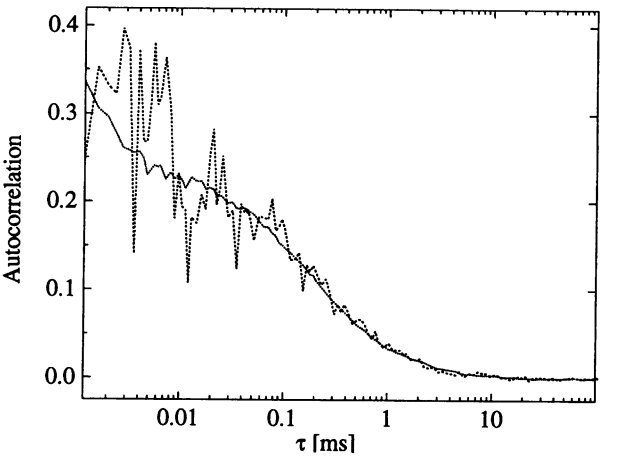

FIGURE 5 Cy-5 excited by the two lasers, autocorrelation curves. *Short dots*: 647-nm excitation; *dots:* 488-nm excitation. It can be seen that amplitudes and characteristic time constants are equal, so it can be assumed that the illuminated volume elements perfectly overlap.

fraction double-labeled DNA, a molecule that is twice as large is observed by auto- and cross-correlation. The functions are normalized to the same N_{tot} to better compare the diffusion times; the original cross-correlation's amplitude differs by 3 times. In the two autocorrelation curves, the more quickly diffusing single strand and the more slowly diffusing double strand are equally represented in the data, whereas in the cross-correlation curve, because of the weighting of a factor of approximately 1:20, the fast component cannot be seen. Therefore, the decay time of the cross-correlation curve, representing the average diffusion time, is larger. The evaluation of the temporal decay by Marquardt fit (Eq. 9; $\Sigma i = 2$ for autocorrelations, $\Sigma i = 1$ for cross-correlation) gives a concentration distribution of [G] ≈ [R] ≈ 3 [GR] for the measured system, where the diffusion times are determined to be $\tau_G \approx \tau_R = 0.65$ ms, $\tau_{GR} = 2$ ms. With calibrated $z_0/r_0 = 5$ as a fixed value, reproducible fits can be performed easily. The reason for the difference of the factor of 3 in the diffusion coefficients of single and double strands may be related to a change in secondary structure of the molecules.

The fraction of fluorophores in the triplet state, given by the fast decay process (τ_T = 1–10 μs) in the correlation curves, especially for Cy-5, is reduced significantly for the cross-correlation, as this can be seen in Fig. 6. This can be explained by the fact that the joint probability that both dyes on a doubly labeled molecule will be in the triplet state is much lower than the probability for either singly labeled molecule. For an extensive discussion of triplet state effects in fluorescence autocorrelation curves, see the publications of Widengren (Widengren et al., 1995). In our FCS applications, the presence of molecules in the triplet state always complicates the numerical evaluation of fast diffusion processes, especially if the triplet relaxation times are considerably large (10-μs range), as in the case of Cy-5. Cross-correlation therefore simplifies the evaluation.

Renaturation experiment

In the renaturation experiment followed by a cross-correlation analysis, the two DNA single strands with rhodamine green and Cy-5 labels, respectively, are mixed together in annealing buffer with equimolar concentrations (here 10 nM). A droplet of this solution is set under the microscope objective and illuminated by the two laser beams as described above. At room temperature and at low concentration, the reaction is very slow and can be followed by FCS measurements over 1 h. The data acquisition times for correlation curves are between 30 s and 120 s; the probe is satisfactorily equilibrated during this time, and integration errors are below 5%. We expect irreversible reaction with

TABLE 1 Photocount efficiency per molecule, determined by FCS

Emission amplitudes	η_{GGG}	η_{RRR}	η_{RGG}	η_{RRG}	η_{RGR}
Photocounts/s per molecule	16,000	14,700	850	1,700	130

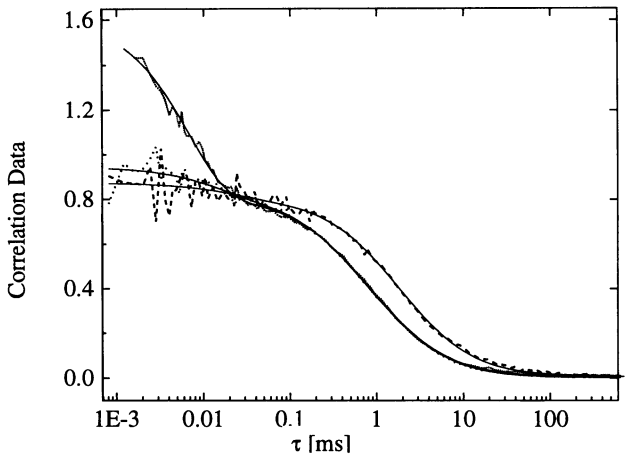

FIGURE 6 Autocorrelation curves and cross-correlation for a mixture of species G, R, and GR, the single labeled in threefold excess against GR. *Short dots:* Autocorrelation of red detection channel; *dots:* autocorrelation of green detection channel; *dashed line:* cross-correlation; *solid lines:* fitting functions. Decay time of the autocorrelations is given by diffusion of fast educt and slow product; the decay time of the cross-correlation is given by the slow product alone and thus is longer.

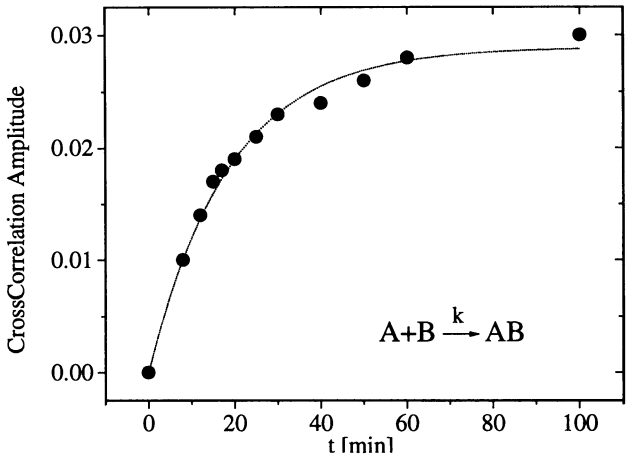

FIGURE 8 Plot of cross-correlation amplitude during the reaction (*points*). The kinetic rate parameter may directly be evaluated from these data. By fitting the irreversible second-order reaction (*short dots*), we get $k = 8 \times 10^5\ M^{-1}\ s^{-1}$.

high association rates, so that species GR does not dissociate in the time scale of analysis. The amount of GR increases with time, reaching a stationary value. Fig. 7 shows the time course of cross-correlation function over 120 min. Fig. 8 shows a plot of the cross-correlation amplitude values versus time. Because the amplitude is proportional to the concentration of the product, the association rate constant can be directly determined from Fig. 8. The value we get by evaluation of the second-order irreversible reaction is $8 \times 10^5\ M^{-1}\ s^{-1}$. The cross-correlation curves can be fitted well with the single-species diffusion model, although the statistical quality is not as high as for autocorrelation curves, because of the higher denominators.

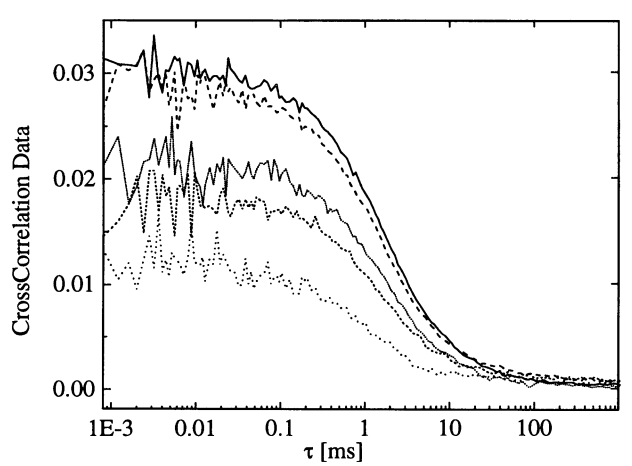

FIGURE 7 Time course of the cross-correlation function in the renaturation (hybridization) reaction. *Light dots:* 8-min incubation; *dots:* 15 min; *short dots:* 25 min; *dashed line:* 60 min; *solid line:* 120 min. The fraction of GR molecules represented by the amplitude increases with time. The diffusion time (curve decay time) remains the same.

DISCUSSION

A dual-color cross-correlation analysis was carried out for a two-component reaction model to follow changes in the product's concentration independently during the progress of the renaturation reaction. Because the investigation of reaction products is of great interest in this type of FCS application, cross-correlation has proved to be an effective aid in separating products from educts. Compared with measurement schemes in which only one educt species is labeled or both educts are labeled with the same dye, the characteristic diffusion of the product is more prevalently represented in the correlation curve than is the diffusion process of the smaller educts. Evaluation of the curves is therefore much easier, because the concentration of product may be directly determined from the amplitude of the cross-correlation curve. With single-color autocorrelation schemes, fitting algorithms and extensive calibration measurements are necessary to extract the same information from an analysis of the average diffusion time.

It has been shown that a two-laser, two-detector device can be used effectively in a confocal FCS setup without extensive experimental changes. The most critical part of the setup is the microscope objective; it must be absolutely free of chromatic aberrations. A helpful means of achieving adequate focal spot is the telescope system for at least one of the two laser beams, although laser pinholes can also be used. The choice of the dye and the filter set is very important for minimizing the cross-talk for nonideal emission characteristics. The values η_i obtained from our measurements may be improved by using narrower filters or dyes with narrower absorption and emission spectra. The major disadvantages in cross-correlation analysis are derived from cross-talk of the dyes and from the denominator of the normalized curve (Eq. 11). Because all fluorescent molecules in the observed volume contribute to the cross-correlation denominator, there is a lower limit to the relative

fraction of detectable product. In the system described here, cross-correlation cannot improve the signal-to-background ratio for systems with a 1000-fold excess of singly labeled species, as expected (Eigen and Rigler, 1994). Carrying out the above measurements with cross-talk of singly labeled educts of 5%, we would not expect the least detectable fraction of doubly labeled product from diffusional evaluation of the cross-correlation curve to be below 1%. However, in equimolar reaction schemes (e.g., nucleic acid renaturation measurements), cross-correlation can be very valuable for making quantitative evaluation of parameters (like diffusion time and fractions in multicomponent systems) much quicker and simpler. In the future, the measurement can be performed with antibody systems, opening up the field of diagnostics for two-color antibody assays for FCS detection. In nucleic acid research, two-color cross-correlation could improve the detection specificity of two DNA probes for their complementary DNA/RNA target sequences by further reducing false-positive signals due to nonspecific binding of either probe. This may provide a large advantage in systems in which the target sequence must be amplified by polymerase chain reaction or by 3SR/NASBA before FCS detection (Walter et al., 1996; Oehlenschläger et al., 1996).

We thank Prof. Manfred Eigen for stimulating discussions; Mareike Lamsbach for preparation and purification of dsDNA; Dr. Andreas Schnetz, Zeiss Oberkochen, for very cooperative meetings; and Dr. Bob Clegg for critical reading of the manuscript.

This work was supported by grant 0310739 from the German Ministry for Education, Science, Research, and Technology. Financial support by EVOTEC BioSystems and an award from the Alexander von Humboldt Foundation to RR are gratefully acknowledged.

REFERENCES

Aragon, S. R., and R. Pecora. 1976. Fluorescence correlation spectroscopy as a probe of molecular dynamics. *J. Chem. Phys.* 64:1791–1803.

Aurup, H., T. Tuschl, F. Benseler, J. Ludwig, and F. Eckstein. 1994. Oligonucleotide duplexes containing 2′-amino-2′-deoxycytidines: thermal stability and chemical reactivity. *Nucleic Acids Res.* 22:20–24.

Berland, K. M., P. T. C So, Y. Chen, W. W. Mantulin, and E. Gratton. 1996. Scanning two-photon fluctuation correlation spectroscopy: particle counting measurements for detection of molecular aggregation. *Biophys. J.* 71:410–420.

Brinkmeier, M., and R. Rigler. 1996. Flow analysis by means of fluorescence correlation spectroscopy. *Exp. Techn. Phys.* 41:205–210.

Ehrenberg, M., and R. Rigler. 1974. Rotational brownian motion and fluorescence intensity fluctuations. *Chem. Phys.* 4:390–401.

Eigen, M., and R. Rigler. 1994. Sorting single molecules: applications to diagnostics and evolutionary biotechnology. *Proc. Natl. Acad. Sci. USA.* 91:5740–5747.

Elson, E. L., and D. Magde. 1974. Fluorescence correlation spectroscopy. I. Conceptual basis and theory. *Biopolymers.* 13:1–27.

Elson, E. L., D. Magde, and W. W. Webb. 1974. Fluorescence correlation spectroscopy. II. An experimental realization. *Biopolymers.* 13:29–61.

Fasman, G. D., editor. 1976. Handbook of Biochemistry and Molecular Biology. CRC Press, Cleveland.

Kam, Z., and R. Rigler. 1982. Cross-correlation laser scattering. *Biophys. J.* 39:7–13.

Kinjo, M., and R. Rigler. 1995. Ultrasensitive hybridization analysis using fluorescence correlation spectroscopy. *Nucleic Acids Res.* 23: 1795–1799.

Koppel, D. E. 1974. Statistical accuracy in fluorescence correlation spectroscopy. *Phys. Rev. A.* 10:1938–1945.

Koppel, D. E., D. Axelrod, J. Schlessinger, E. L. Elson, and W. W. Webb. 1976. Dynamics of fluorescence marker concentrations as a probe of mobility. *Biophys. J.* 16:1315–1329.

Magde, D., E. L. Elson, and W. W. Webb. 1972. Thermodynamic fluctuations in a reacting system—measurement by fluorescence correlation spectrocsopy. *Phys. Rev. Lett.* 29:705–708.

Magde, D., E. L. Elson, and W. W. Webb. 1978. Fluorescence correlation spectroscopy. III. Uniform translation and laminar flow. *Biopolymers.* 17:361–376.

Oehlenschläger, F., P. Schwille, and M. Eigen. 1996. Detection of HIV-1 RNA by nucleic acid sequence-based amplification combined with fluorescence correlation spectroscopy. *Proc. Natl. Acad. Sci. USA.* 93: 12811–12816.

Palmer, A. G., and N. Thompson. 1987. Molecular aggregation characterized by high order autocorrelation in fluorescence correlation spectroscopy. *Biophys. J.* 52:257–270.

Petersen, N. O. 1986. Scanning fluorescence correlation spectroscopy. I. Theory and simulation of aggregation measurements. *Biophys. J.* 49: 809–815.

Qian, H., and E. L. Elson. 1991. Analysis of confocal laser-microscope optics for 3-D fluorescence correlation spectroscopy. *Appl. Opt.* 30: 1185–1195.

Rauer, B., E. Neumann, J. Widengren, and R. Rigler. 1996. Fluoresence correlation spectrometry of the interaction kinetics of tetramethylrhodamin α-bungarotoxin with *Torpedo californica* acetylcholine receptor. *Biophys. Chem.* 58:3–12.

Ricka, J., and T. Binkert. 1989. Direct measurement of a distinct correlation function by fluorescence cross correlation. *Phys. Rev. A.* 39: 2646–2652.

Rigler, R., and Ü. Mets. 1992. Diffusion of single molecules through a Gaussian laser beam. *Soc. Photo-Opt. Instrum. Eng.* 1921:239–248.

Rigler, R., Ü. Mets, J. Widengren, and P. Kask. 1993. Fluorescence correlation spectroscopy with high count rates and low background: analysis of translational diffusion. *Eur. Biophys. J.* 22:169–175.

Rigler, R., and J. Widengren. 1990. Ultrasensitive detection of single molecules by fluorescence correlation spectroscopy. *Bioscience.* 3:180–183.

Rigler, R., J. Widengren, and Ü. Mets. 1992. Interactions and kinetics of single molecules as observed by fluorescence correlation spectroscopy. *In* Fluorescence Spectroscopy. O. S. Wolfbeis, editor. Springer, Berlin. 13–24.

Schwille, P., F. Oehlenschläger, and N. Walter. 1996. Quantitative hybridization kinetics of DNA probes to RNA in solution followed by diffusional fluorescence correlation analysis. *Biochemistry.* 35:10182–10193.

v. Smoluchowski, M. 1916. Zusammenfassende Bearbeitungen. *Physik. Z.* 17:557–585.

Thompson, N. L. 1991. Fluorescence correlation spectroscopy. *In* Topics in Fluorescence Spectroscopy, Vol. 1. J. R. Lakowicz, editor. Plenum Press, New York. 337–378.

Tong, P., K.-Q. Xia, and B. J. Ackerson. 1993. Incoherent cross-correlation spectroscopy. *J. Chem. Phys.* 89:9256–9265.

Walter, N., P. Schwille, and M. Eigen. 1996. Fluorescence correlation analysis of probe diffusion simplifies quantitative pathogen detection by PCR. *Proc. Natl. Acad. Sci. USA.* 93:12805–12810.

Widengren, J., Ü. Mets, and R. Rigler. 1995. Fluorescence correlation spectroscopy of triplet states in solution: a theoretical and experimental study. *J. Chem. Phys.* 99:13368–13379.

Widengren, J., R. Rigler, and Ü. Mets. 1994. Triplet-state monitoring by fluorescence correlation spectroscopy. *J. Fluoresc.* 4:255–258.

Xia, K.-Q., Y.-B. Xin, and P. Tong. 1995. Dual-beam incoherent cross-correlation spectroscopy. *J. Opt. Soc. Am. A.* 12:1571–1778.